Hindawi
Shock and Vibration
Volume 2021, Article ID 4540252, 13 pages
https://doi.org/10.1155/2021/4540252

Research Article

Evaluation of Failure Probability in Series System of Three-Axle Trucks under Strong Crosswind

Yahui Hu,[1] **Yingshi Guo**,[1,2] **Rui Fu**,[1,2] **and Qingjin Xu**[1]

[1]*School of Automotive Engineering, Chang'an University, Xi'an, China*
[2]*Key Laboratory of Automobile Transportation Safety Technology, Chang'an University, Xi'an, China*

Correspondence should be addressed to Yingshi Guo; guoys@chd.edu.cn

Received 14 April 2021; Revised 14 July 2021; Accepted 2 August 2021; Published 14 August 2021

Academic Editor: Zengshun Chen

The probability of wind-induced failure accidents in three-axle trucks under pulsating strong crosswinds and the corresponding critical safe speed are investigated in this study. Reliability theory and random fuzzy methods are utilized to establish the membership function of the failure probability in the series system (FPSS) composed of rollover, side-slip, and rotation failure accidents. The Kaman spectrum is used to realistically simulate the fluctuating wind time history curves of different average speeds. Four factors affecting the six-component force coefficient of the three-axle truck and the crosswind load are considered: fluctuating average wind speed, wind direction (angle), truck driving speed, and road adhesion coefficient. A three-axle truck nonlinear model is established accordingly. The model is used to obtain the dynamic response of the three-axle truck under strong crosswind conditions as per the time-varying curves of the vertical load of the truck, the time-varying curves of the lateral displacement of the center of mass, and the time-varying curves of the heading angle. An advanced Monte Carlo simulation algorithm based on importance sampling is used to determine the probability of a three-axle truck with FPSS under strong crosswinds; the given acceptable probability of failure (accident) is used to obtain the critical safety speed. The sensitivity analysis of random variables reveals that the possibility of three truck failures of the three-axle truck in strong crosswinds is, from largest to smallest, rollover, side-slip, and rotation. This research may provide useful guidance for exploring the probability of wind-induced accidents and the critical safety speeds of vehicles, as well as useful general information for road transportation management departments.

1. Introduction

Advancements in the transportation industry have created massive, highly complex road transportation networks. Safety is a critical concern in the operation of these networks, which are characterized by strong crosswinds, which can cause accidents in large vehicles such as trucks. Strong crosswind accidents are not common, but they can be extremely serious when they do occur [1]. Any vehicle encountering strong crosswinds can experience serious side-slipping, rotation, and/or rollover failure due to magnification of the terrain [2]. It is important to fully understand the characteristics of vehicles traversing strong crosswind environments to keep roadways and drivers safe.

Several methods have been proposed to reduce the impact of strong crosswinds on vehicles such as wind barriers, certain vehicle designs, and strengthened driver training [3]. Wind barriers may reduce the occurrence of wind-induced accidents, but they are too costly to install in large volumes [4] and thus do not unsatisfactorily prevent wind-induced accidents. A strong crosswind warning system can be established to target drivers for enhanced safety. For example, previous scholars [2] have divided strong crosswinds into various risk levels to suggest specific target speeds to drivers that may reduce the probability of wind-induced accidents. Road transportation management departments also monitor strong crosswinds and may close certain roads if the wind speeds moving across them exceed certain

thresholds. In this regard, the need for a reasonable evaluation of wind-induced accident probability is particularly important.

Many previous researchers have analyzed the stability of road-traversing vehicles and the probability of wind-induced accidents. Many have used numerical simulations to study the stability of vehicles encountering strong crosswinds; many others have used wind tunnels to test the six-component force coefficients of vehicles [5–7]. Chen et al. provide a reference for the unsteady aerodynamic characteristics of the air fluid around a cone-shaped building and conducted wind tunnel experiments on irregular buildings [8–10]. Dynamic models of natural winds and vehicles are strongly nonlinear. The probability of wind-induced accidents on vehicles is closely related to the specific type of vehicle, and wind tunnel operation is extremely expensive. Wind tunnel testing is often impractical, so numerical simulations are accepted by many researchers. However, when using numerical simulation to evaluate vehicle stability, the accuracy of the results is contingent on the specific model being utilized. A high-precision, multibody dynamics model should be established to counteract the nonlinearity of the dynamic characteristics of vehicles. The six-component force coefficient acting on vehicles not only changes with the highly random crosswind conditions at hand, but also closely depends on the shape of the vehicle. In most studies, crosswinds are treated as unsteady processes (which remits extremely low accuracy) [11].

In order to study the stability of road-traversing vehicles under crosswind conditions, Baker [12] established an artificially generated steady-state crosswind as the vehicle excitation; however, this model has extremely low accuracy. Baker [13] further conducted an in-depth study on the safety of vehicles subjected to strong crosswinds by expanding the dynamic model used in previous studies and defined three failure modes accordingly: rollover accident, side-slip accident, and rotation accident. Parameters including the position of the center of mass and mass of the vehicle, as well as aerodynamics, also significantly impact the crosswind stability of a given vehicle.

Chen and Cai [14, 15] analyzed the stability of vehicles crossing long-span bridges under the influence of crosswinds, established a vehicle-bridge coupling model, and explored the dynamic relationship between vehicles accordingly. This vehicle-bridge-wind coupling system not only is an essential framework for evaluating the stability of trucks under strong crosswinds, but also is an approach towards calculating the critical safety speed of vehicles [16–19].

Nonstationary wind gust and turbulence models are often utilized with random variables. Widely recognized gust models include "1 − cos" [20, 21], "Chinese hat" [22], and "rugby-ball" [23]. Despite many valuable contributions to the literature, the stability of vehicles in crosswind conditions is not yet fully understood. Previous studies on this subject have mostly used deterministic methods, but the results obtained by these methods are often conservative [24]; overly conservative variables can cause vehicles to travel too slowly and cause traffic congestion. Deterministic methods do not incorporate the influence of other random factors, which makes their results unreliable.

Snæbjornsson et al. [25] adopted a probability model based on reliability theory to evaluate the stability of vehicles in strong crosswinds; their model was shown to outperform deterministic methods. Wetzel and Proppe [26] used a method similar to that of a previous researcher [25] to determine the probability of wind-induced failure in vehicles and also conducted a sensitivity analysis of random variables as a supplementary measure. The literature does contain workable examples for the use of probabilistic methods to assess the probability of wind-induced vehicle failure, but previous scholars have not considered the nonsteady characteristics of crosswinds when making their predictions. The random and unsteady characteristics of crosswinds should be considered to evaluate them more realistically.

Additionally, only one of the three failure modes can typically be simulated at a time. However, the nonlinearity of vehicle dynamics and the strong uncertainty of crosswinds make it impossible to realistically predict which of the three failure modes will occur (though all three can be defined as an "accident"). Such cases can be referred to as "series system failure," where the failure probability is the "failure probability of the serial system" (FPSS).

The probability of wind-induced accident occurrence for trucks and the corresponding critical safety speed were simulated and analyzed in this study. The random uncertainty of crosswinds, random wind speed, random wind angle, random driving speed of trucks, and random road adhesion coefficient were taken into account. Based on the reliability theory, the random fuzzy method is used to simulate FPSS and calculate the acceptable threshold of failure probability for the critical safety speed of trucks under a given crosswind speed (or the critical crosswind speed that the truck can withstand). The results of this work may provide a sound theoretical basis for transportation management departments to minimize wind-induced failure of trucks on their roadways.

The remainder of this paper is organized as follows. Section 2 introduces the reliability modeling theory and method. Section 3 introduces the gust model and wind load simulation method. Section 4 presents the three-axle truck dynamic model and selection of parameters. Section 5 discusses the fuzzy random method based on importance sampling. Section 6 gives the results of the simulation based on the proposed method. Section 7 provides a brief summary and concluding remarks.

2. Reliability Modeling Method

2.1. Based on Reliability Theory. Reliability theory is a relatively traditional method for calculating the failure probability of a system, which requires clear, precise parameters. Similarly, when using this theory to evaluate vehicle stability under crosswind conditions, given the driving speed of a vehicle, the maximum instantaneous wind speed of natural wind is the speed $\widehat{w}$ of the crosswind. The direction of the incoming flow of the crosswind and the driving direction of the vehicle are characterized by the angle of attack α. When

using this deterministic method to calculate vehicle stability, the final output result is the maximum wind speed that the vehicle can resist when it does not roll over, slip, or rotate at a given driving speed and angle of attack [27, 28]. This can be expressed as follows:

$$\widehat{w} = f(v, \alpha). \tag{1}$$

However, when the reliability theory is used to analyze the failure probability of road-traversing vehicles under crosswind conditions, the system parameters that affect stability are often uncertain. The natural wind speed w can be considered to be composed of an average wind speed $\overline{w}$ and an uncertain random wind speed $w\prime$. In previous studies, the average wind speed was usually treated as a stable value, while random wind speed was considered to have a Gaussian distribution with a mean value of zero. This does not properly reflect the randomness of wind speed. Taking into account the uncertainty of these system parameters, it is usually impossible to determine whether a vehicle is safe under a given condition; only the probability Pf of an accident under a given condition can be calculated.

Here, the uncertainty parameter is treated as a random variable represented by $X = (X_1, X_2, \ldots, X_m)$. Given the vehicle speed, average wind speed, and angle of attack, the probability of a vehicle accident P_f can be calculated as follows:

$$P_f = P_f(X, v, \overline{w}, \alpha). \tag{2}$$

When the reliability method is used to calculate the probability of a vehicle accident, the vehicle speed, average wind speed, and angle of attack are all definite parameters. Therefore, once the random variable X has been determined, it can be expressed by the parameters $v, \overline{w}, \alpha, \varphi$ and equation (2) can be rewritten as

$$P_f = P_f(v, \overline{w}, \alpha, \varphi). \tag{3}$$

The average wind speed can be expressed as

$$\overline{w} = \overline{w}\left(v, P_f, \alpha, \varphi\right). \tag{4}$$

Equation (4) describes the maximum average wind speed that a vehicle can resist under the condition of an acceptable failure probability. This is a probabilistic wind characteristic curve (PCWC) [29]:

$$\overline{w} = PCWC\left(v, P_f, \alpha, \varphi\right). \tag{5}$$

2.2. Definition of Vehicle Failure State. Before evaluating the operational safety of vehicles under crosswind conditions on large bridges, it is first necessary to define the standards for different vehicle failure modes. The current state of the vehicle itself must be considered as well as the safety impact of the current vehicle on other vehicles in the traffic flow. For example, consider a vehicle traveling on a long bridge that is advancing along the bridge deck, where it suddenly encounters interference due to crosswinds. The driver then quickly adjusts his or her current driving state to attempt to regain stability and avoid a collision. The traffic flow in this state is highly complex, so it is necessary to clearly define the standards for different failure modes of different vehicles.

According to Baker [7], when analyzing the safety of vehicles driving on a bridge under crosswind conditions, the failure modes include the side-slip accident, rotation accident, and rollover accident.

(1) A side-slip accident refers to the lateral displacement of the vehicle reaching or exceeding 0.5 m, namely,

$$y(t) \geq y_{\max} = 0.5, \tag{6}$$

where $y(t)$ refers to the actual lateral displacement of the center of mass of the vehicle disturbed by a crosswind in the time domain, while $y_{\max} = 0.5$ m represents the critical value of the vehicle's side-slip accident. When $y(t)$ reaches 0.5 m, the vehicle experiences a side-slip accident.

(2) A rotation accident refers to the rotation of the center of mass of the vehicle around the z-axis fixed in the vehicle coordinate system causing the heading angle of the vehicle to be greater than 0.2 rad, namely,

$$r(t) \geq r_{\max} = 0.2, \tag{7}$$

where $r(t)$ refers to the heading angle of the vehicle in the current state and $r_{\max} = 0.2$ rad represents the critical value of the accident. When the heading angle of the vehicle reaches 0.2 rad, the vehicle experiences a rotation accident.

(3) A rollover accident is defined by the so-called load transfer ratio (LTR):

$$\mathrm{LTR} = \left|\frac{F_{Rz} - F_{Lz}}{F_{Rz} + F_{Lz}}\right|, \tag{8}$$

where F_{Rz} and F_{Lz}, respectively, represent the vertical tire force of the left and right wheels of the vehicle. An LTR value between 0 and 1 is considered safe.

The above three failure modes can be used to evaluate vehicle failure probabilities in various scenarios. Under extreme conditions (e.g., extremely high crosswind speeds), the vehicle may fail even if it is moving at an extremely low speed or is stationary.

2.3. Introduction to Fuzzy Random Method. According to the reliability theory (Section 2.1) and vehicle failure state classifications (Section 2.2) given above, the failure probability of vehicles under crosswind conditions can be calculated. The random function Z is defined here as the function of the system:

$$Z = g_x(X) = g_x\left(X_1, X_2, \ldots, X_m\right). \tag{9}$$

In the traditional reliability analysis model, $Z = 0$ usually indicates that the system is in the boundary state of failure and safety; $Z > 0$ usually indicates that the system is in a safe

state; and $Z < 0$ usually indicates that the system is in a failure state.

The failure state and safety state of the system in an actual reliability analysis problem typically do not have a clear boundary, but rather have fuzzy characteristics. In this case, $Z = 0$ is not defined as an accurate failure state or a boundary condition of a reliable state. A transition state can be set between the failure state and the reliable state to range within $[Z_f, Z_r]$. Under normal circumstances, when $Z \le Z_f$, the system is considered to be in a complete failure state. When $Z_r \le Z$, the system can be considered to be in a completely reliable state. When $Z_f < Z < Z_r$, it is in an intermediate fuzzy state.

Considering that X is a random variable, and judging Z as in a certain state, the criterion for predicting the failure of vehicles is fuzzy. The fuzzy event that occurs in any one of the three failure modes is denoted as E, where a failure (accident) has occurred in the vehicle system. Assuming that the joint probability density function of the random variable X is $f_x(X)$, the performance function is $g_x(X)$ and the failure probability of the vehicle system is

$$P_f = P(E) = \int_{R^n} \mu_E[g_x(X)] f_x(X) \mathrm{d}x, \tag{10}$$

where $\mu_E[g_x(X)]$ represents the membership function.

2.4. Performance Function and Membership Function Determination. Equation (10) expresses the probability of failure of the vehicle system. Performance function $g_x(X)$ and membership function $\mu_E[g_x(X)]$ must be determined before conducting this calculation.

In order to analyze the operational safety of vehicles exposed to crosswinds, the performance function must be related to the three failure modes. In the stability analysis of traditional high-speed trains under crosswind conditions, the load transfer rate is used to express stability. The load transfer rate widely used in China is 0.8, which is equivalent to a 20% safety margin for the operation of high-speed trains. Without loss of generality, when calculating the failure probability of different vehicle failure modes, a corresponding safety margin of 20% is appropriate. The safety indicators for different vehicle failure modes are redefined here accordingly.

The side-slip accident can be defined by the ratio of the side-slip displacement to the maximum allowable side-slip displacement, or rate of side-slip (RS):

$$\mathrm{RS}(X, v, \overline{w}, \alpha, \phi) = \left| \frac{y(t)}{y_{\max}} \right|. \tag{11}$$

The rotation accident can be defined by the ratio of the rotation accident rotation angle to the maximum rotation angle, or the rate of rotation (RR):

$$\mathrm{RR}(X, v, \overline{w}, \alpha, \phi) = \left| \frac{r(t)}{r_{\max}} \right|. \tag{12}$$

Rollover accidents are defined by the load transfer ratio (LRT):

$$\mathrm{LTR}(X, v, \overline{w}, \alpha, \varphi) = \left| \frac{F_{Rz} - F_{Lz}}{F_{Rz} + F_{Lz}} \right|. \tag{13}$$

The function of the vehicle system is

$$g_x(X) = \min\{g_x(X)\} = \min\{1 - \mathrm{RS}, 1 - \mathrm{RR}, 1 - \mathrm{LTR}\}. \tag{14}$$

The structural risk of vehicles increases as Z decreases, and the membership function $\mu_E[g_x(X)]$ should also be a decreasing function of Z, so a semi-trapezoid is adopted here. The semi-trapezoid shape is expressed as follows as a membership function of vehicle structure reliability analysis:

$$\mu_E[g_x(X)] = \begin{cases} 0, & Z \le Z, \\ \dfrac{Z_u - Z}{Z_u - Z_l}, & Z_l < Z \le Z_u, \\ 1, & Z_u < Z. \end{cases} \tag{15}$$

When using reliability theory to analyze the failure probability of high-speed trains, it is generally considered that the operating state of high-speed trains is reliable when the load transfer rate (LTR) does not exceed 0.8. Without loss of generality, when calculating the reliability of road-traversing vehicles, RS, RR, and LRT are safe when they do not exceed 0.8. The corresponding membership function is 1 and the running state of the vehicle is reliable. When RS, RR, and LRT reach 0.8, the corresponding membership function is 0, and the vehicle is in a failed state. The fuzzy boundary range of the membership function is 0 and 0.2; that is, Z_l and Z_u are 0 and 0.2, respectively.

3. Gust Model and Wind Load

3.1. Introduction to the Pulsating Wind Model. Many previous researchers [2, 17, 24, 30, 31] have stated that random crosswinds consist of two parts: average wind $\overline{w}$ and pulsating wind $w\prime$. Thus,

$$w = \overline{w} + w' \tag{16}$$

Pulsating wind originates from three directions. The strongest influence on vehicle stability among the three directions of pulsating wind is the incoming flow [32, 33]. Numerical values are adopted here to simplify the calculation model in incorporating the effects of pulsating wind direction on the stability and reliability of vehicles.

It is assumed that the vehicle is traveling along the road in a random wind field at a speed v. The relative speed of the direction of the pulsating wind flow relative to the vehicle needs to be calculated. Cooper [35] proposed a random process for vehicles traveling in random turbulence and established a dimensionless power spectral density definition [35] that is widely used by researchers [36–38]:

$$\frac{nS_w}{\sigma_w^2} = \left[\frac{4\lambda}{\left(1+70.8\lambda^2\right)^{5/6}}\right] \times \left[M_u^2 + \left(1-M_u^2\right)\frac{0.5+94.4\lambda^2}{1+70.8\lambda^2}\right], \tag{17}$$

where

$$\lambda = \frac{nL\prime}{\overline{u}}, \tag{18}$$

$$M_u^2 = \left[\frac{v\cos\alpha + \overline{w}}{\overline{u}}\right]^2, \tag{19}$$

$$\overline{u} = \mathrm{sqrt}\left(v^2 + \overline{w}^2 + 2v\overline{w}\cos\alpha\right). \tag{20}$$

However, in formula (19),

$$L\prime = \mathrm{sqrt}\left[{}^{x}Lw\left(M_u^2 + 4\left(\frac{{}^{y}Lw}{{}^{x}Lw}\right)^2\left(1-M_u^2\right)\right)\right]. \tag{21}$$

The left side of the equal sign in equation (17) represents the dimensionless power spectral density, n represents the corresponding frequency, S_w represents the power spectral density of the wind, σ_w^2 represents the variance of the fluctuating wind, and the slight turbulence of the fluctuating wind is expressed by I_Z. The relationship between the variance of fluctuating wind and the intensity of turbulence is

$$\begin{aligned}\sigma_w &= I_z\overline{w},\\ I_z &= \frac{\left(1-\left(1/\left(2\times10^4\right)\right)\right)\left(\lg\left(20h_0\right)+2\right)^7\right)}{\ln\left(z/z_0\right)},\end{aligned} \tag{22}$$

where z_0 represents ground roughness length. According to public information, the values of z_0 and z are generally 0.07 m and 4 m [36], respectively.

The length of the turbulence integral in the transverse and longitudinal directions can be determined by

$$\begin{cases} L_w = 50\times\dfrac{z^{0.35}}{z_0^{0.063}}, & w = 0.42^{x}Lw.\\ {}^{y}L \end{cases} \tag{23}$$

In previous studies [39, 40], the power spectrum density at several discrete frequencies was superimposed to simulate fluctuating wind:

$$w\prime = \sum_j \sqrt{2S_w\left(n_j\right)\Delta n_j}\sin\left(2\pi n_j t + 2\pi r_j\right), \tag{24}$$

where t represents the simulation time, n_j represents the discrete frequency, Δn_j represents the frequency step size at the discrete frequency, and r_j is an automatically generated random number between 0 and 1.

3.2. Calculation of Unsteady Aerodynamic Load. As discussed in Section 3.1, random wind is composed of average wind and pulsating wind. The unsteady aerodynamic load F should also consist of two parts: the average load caused by the average wind $\overline{F}$ and the pulsating load $F\prime$ caused by the pulsating wind. The superposition of these two load parts is the quasisteady air load.

$$F = \overline{F} + F\prime = 0.5\rho A_v C_F(\beta)\left(\overline{u}+u\prime\right)^2, \tag{25}$$

where ρ represents the air density, A_v represents the windward reference area, $C_F(\beta)$ represents the aerodynamic coefficient, and β represents the yaw angle. Formula (25) is suitable for calculation of aerodynamic load at a fixed point in the air, but when calculating the stability of vehicles under actual in a crosswind conditions, the vehicle's speed must be considered. The change of yaw angle caused by Taylor series is used to obtain the aerodynamic coefficient:

$$C_F(\beta) = C_F(\overline{\beta}) + C_F'(\overline{\beta})(\beta-\overline{\beta}). \tag{26}$$

To simplify formula (26), $C_F(\overline{\beta})$ is written as $\overline{C}_F$, $C_F'(\overline{\beta})$ as $\overline{C}_F'$, and $(\beta-\overline{\beta})$ at the same time as $\beta\prime$. The average aerodynamic coefficient can be obtained as

$$\overline{F} = 0.5\rho A_v\overline{C}_F\overline{u}^2. \tag{27}$$

Assuming that the parameters $u\prime$ and $\beta\prime$ are very small, formula (25) can be rewritten to obtain the time-varying aerodynamic coefficient $F\prime$ according to the first-order expansion:

$$F\prime = 0.5\rho A_v C_F'\overline{u}^2\beta\prime + \rho A_v\overline{C}_F\overline{u}u\prime. \tag{28}$$

Calculating the relative speed of the air relative to the vehicle, as shown schematically in Figure 1, includes the traveling speed v of the vehicle, random wind speed w, and wind attack angle α. According to the geometric relationship in Figure 1,

$$\overline{u}^2 = \left(v+\overline{w}\cos\alpha\right)^2 + \left(\overline{w}\sin\alpha\right)^2, \tag{29}$$

$$u^2 = \left(v+\left(\overline{w}+w\prime\right)\cos\alpha\right)^2 + \left(\left(\overline{w}+w\prime\right)\sin\alpha\right)^2. \tag{30}$$

The relative angle between the crosswind and the vehicle (yaw angle) is expressed as

$$\begin{aligned}\tan\overline{\beta} &= \frac{\overline{w}\sin\alpha}{\left(v+\overline{w}\cos\alpha\right)},\\ \tan\beta &= \frac{\overline{w}\sin\alpha + w\prime\sin\alpha}{\left(v+\overline{w}\cos\alpha + w\prime\cos\alpha\right)}.\end{aligned} \tag{31}$$

Assuming that the pulsation term$w\prime$is extremely small, formula (30) can be simplified as

$$u^2 = \overline{u}^2 + 2\left(v\cos\alpha + \overline{w}\right)w\prime. \tag{32}$$

The expression of the pulsating term $u\prime$ about u and $\overline{u}$ is

$$u\prime = u - \overline{u} = \overline{u}\left(\sqrt{1+\frac{2\left(v\cos\alpha+\overline{w}\right)w\prime}{\overline{u}^2}} - 1\right). \tag{33}$$

Taylor series processing of formula (33) yields

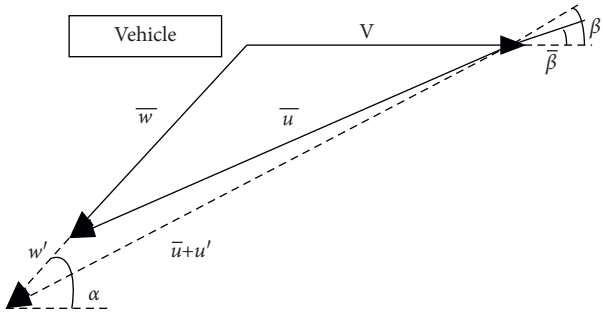

Figure 1: Schematic diagram of relative wind speed.

$$u\prime = \overline{u}\left(\frac{(v\cos\alpha + \overline{w})w\prime}{\overline{u}^2}\right) = \frac{(v\cos\alpha + \overline{w})w\prime}{\overline{u}}. \tag{34}$$

According to the relationship among the pulsation terms $\beta\prime$, β, and$\overline{\beta}$, and assuming that $\beta\prime$ is extremely small,

$$\beta\prime = \tan(\beta - \overline{\beta}) = \frac{vw\prime\sin\alpha}{\overline{u}^2 + (v\cos\alpha + \overline{w})w\prime}. \tag{35}$$

Taylor series processing of formula (35) yields

$$\beta\prime = \frac{vw\prime\sin\alpha}{\overline{u}^2} \tag{36}$$

Substituting formulas (34) and (36) into formula (28) provides the simplified fluctuating air load $F\prime$:

$$F\prime = \rho A_v\left(\overline{C}_F\overline{w} + \left(\overline{C}_F\cos\alpha + 0.5\overline{C}_F'\sin\alpha\right)v\right)w\prime. \tag{37}$$

The above process can be used to determine the quasistatic process of aerodynamic loads. However, the hypothetical quasistatic process may not completely reflect the actual process, because the dimensions calculated for the turbulence integral may not be consistent with the exposed dimensions of vehicles. A weighting function [41] can be used to remedy this:

$$\begin{aligned} F\prime = {} & \rho A_v\left(\overline{C}_F\overline{w} + \left(\overline{C}_F\cos\alpha + 0.5\overline{C}_F'\sin\alpha\right)v\right) \\ & \int_0^\infty g_F(\tau)w\prime(t-\tau)\mathrm{d}\tau, \end{aligned} \tag{38}$$

where $g_F(\tau)$ is the aerodynamic weighting function, and t denotes time.

Without loss of generality, it is also true that the aerodynamic load factor in formula (38) can be replaced by the aerodynamic load moment factor. The substitution is made in formula (38) and then multiplied by the corresponding action height H to determine the unsteady aerodynamic load moment.

It is further necessary to determine the weight parameter $g_F(\tau)$ and aerodynamic coefficient C_F in formula (38). Baker [7] conducted a series of wind tunnel tests to obtain the aerodynamic weight function as follows:

$$g_F(\tau) = \left(\frac{2\pi\overline{n}\prime\overline{u}}{L\prime}\right)^2\tau\exp\left(\frac{2\pi\overline{n}\prime\overline{u}}{L\prime\tau}\right), \tag{39}$$

where $\overline{n}\prime = \lambda\sin\overline{\beta}$. When calculating the lateral force and lifting force, the value of λ is 2.0 or 2.5, respectively.

The aerodynamic coefficient can be obtained through wind tunnel tests or through numerical simulations. Previous researchers [30] simulated aerodynamic coefficients under different yaw angles for vehicles encountering strong crosswinds including the lateral force coefficient C_{Fs}, lift coefficient C_{Fl}, roll moment coefficient C_{Mr}, yaw angle moment coefficient C_{My}, and pitching moment coefficient C_{Mp}. Baker [7], and later, Coleman and Baker [42], determined the aerodynamic coefficient of vehicles in a wind field environment as per the changes in yaw angle:

$$\begin{cases} C_{Fs}(\beta) = 2.55\beta^{0.382}, \\ C_{Fl}(\beta) = 0.40(1+\sin 3\beta), \\ C_{F_D}(\beta) = -0.25(1+2\sin 3\beta), \\ C_{My}(\beta) = -2.0\beta^{1.77}, \\ C_{Mp}(\beta) = 2.6\beta^{1.32}, \\ C_{Mr}(\beta) = 2.7\beta^{0.294}. \end{cases} \tag{40}$$

3.3. Random Variables. The variables affecting the failure probability of vehicles under the influence of crosswinds were investigated in this study. The average speed of pulsating wind, wind angle, truck speed, and road adhesion coefficient were taken into account. The average speed of fluctuating wind was defined as 10 m·s^{-1}, 20 m·s^{-1}, 30 m·s^{-1}, and 40 m·s^{-1}, and the wind angle was set to 0°, 30°, 60°, 90°, 120°, and 150°. The speed of vehicles was 72 kph, 90 kph, 108 kph, 126 kph, or 144 kph. The road adhesion coefficient φ of dry, slippery, snowy, and icy roads was set to 0.8, 0.6, 0.4, and 0.2, respectively.

Fluctuating wind speed is treated here as a random variable; it typically conforms to a stable Gaussian distribution [24]. Through the harmonic superposition method described above, the Kaman spectrum was utilized to construct the crosswind power spectrum and simulate the crosswinds via harmonic superposition. The average wind speed was, respectively, 10 m·s^{-1}, 20 m·s^{-1}, 30 m·s^{-1}, and 40 m·s^{-1} over a fluctuating wind time history curve.

A large number of data samples are necessary to construct a realistic time history curve of pulsating wind. Yu et al. [31] stated that 200 sample data are sufficient. In this study, 1,000 sample simulations of fluctuating winds with different average speeds were utilized. The time history curve with average wind speed of 20 m·s^{-1} is shown in Figure 2. Figure 3 shows a comparison between the simulated power spectrum and calculated power spectrum.

As shown in Figure 2, the time history curve of pulsating wind has strong time-variability in terms of the amplitude and direction of pulsating wind. As shown in Figure 3, the simulated pulsating wind power spectrum is consistent with the target spectrum on the whole. Thus, the pulsating wind power spectrum simulated in this study is reliable.

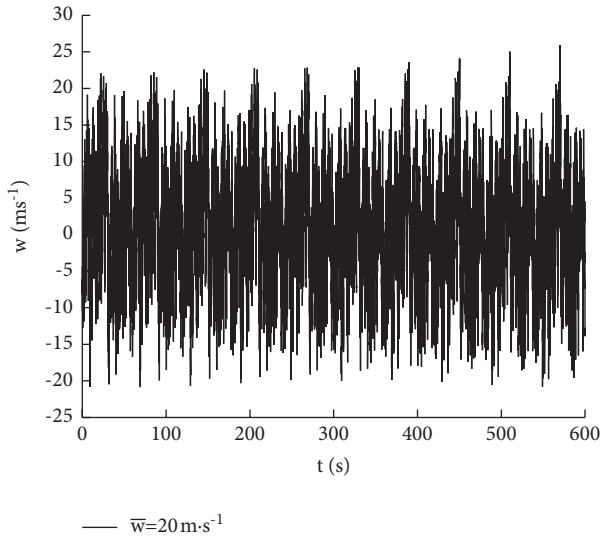

Figure 2: Pulsation crosswind time history curve.

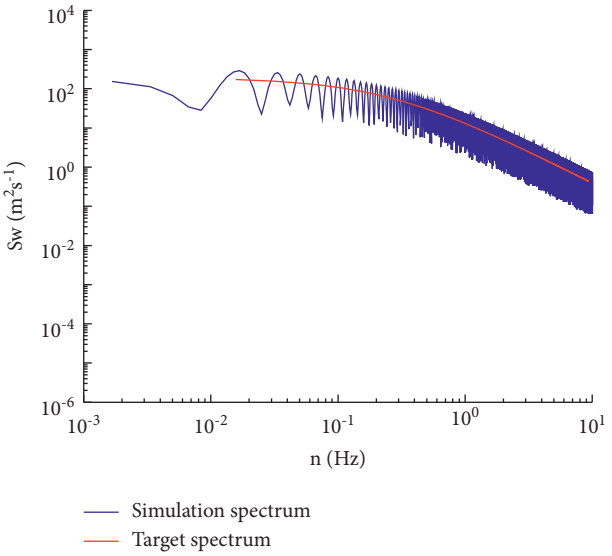

Figure 3: Power spectral density.

4. Road Vehicle Dynamics Model

Kim et al. [6] found that trucks are more susceptible to failures caused by crosswinds. Maybe trucks have larger height than other vehicles and thus experience larger crosswind-ward areas, making them more susceptible to such conditions. Commercial software TruckSim (v2016.1, Mechanical Simulation Corporation [43]) was utilized in this study to establish a truck dynamics simulation model. The software can be used to analyze trucks as well as vans, buses, and passenger cars corresponding to complicated environments such as suspension assemblies, steering systems, power systems, braking systems, and driving behavior systems with interactive mechanisms. TruckSim uses feature-oriented parametric modeling methods to simulate light trucks, buses, heavy semi-trailers, heavy trucks, multiaxle military vehicles, and asymmetrical steering system (multiaxle and single-axle), as well as the responses of multiple trailers and other vehicles affecting driver manipulation (steering, braking, and acceleration) over 3D road surfaces. The aerodynamic input is mainly used to predict handling stability, braking, smoothness, power, and economy across entire vehicles.

4.1. Truck Model Selection. A common three-axle truck traversing a domestic road was constructed in TruckSim with the software's built-in model parameters (Table 1). The aerodynamic parameters of the truck follow the values given by Baker [7], as shown in Figure 4.

4.2. Force Analysis of Truck Tires under the Influence of Pulsating Wind. According to the aerodynamic parameter formula provided by Baker [7], pulsating wind and truck speeds affect the tire force of the truck. Wind speeds of 10 m·s−1, 20 m·s−1, 30 m·s−1, and 40 m·s−1 with vehicle speeds of 72 kph, 90 kph, 108 kph, and 126 kph were simulated in TruckSim with varying wind speeds of 10 m/s and 5 m/s. The change of vertical contact force of the wheels at 144 kph on the platform straight road surface was observed ($\varphi = 0.8$, $\beta = 30^{\circ}$), as shown in Figure 5. Figures 6(a)–6(d) show the changes in vertical tire force under different wind speeds and vehicle speeds. The vehicle speed changes appear to have less effect on the vertical tire force than wind speed. Further, the vertical force of the rear axle tires increases as the wind speed increases. Changes in wind speed have a greater impact on the vertical force of the rear axle tires than the front axle tires; the vertical force of the rear axle tires appears to be zero even at relatively high wind and vehicle speeds. To this effect, the truck is prone to rollover accidents when running in unsafe conditions.

4.3. Lateral Displacement of Trucks under Crosswind Conditions. According to the vehicle safety indicators defined by Baker [7], a side-slip accident will occur in the crosswind environment when the lateral displacement of the truck reaches 0.5 m. The lateral displacement of the truck is related to the crosswind speed, traveling speed of the truck, wind direction (angle), and road adhesion coefficient. The lateral displacement observed in TruckSim with average wind speed of 10 m·s^{-1} or 30 m·s^{-1}, truck traveling speed of 72 kph or 108 kph, wind angle of 30° or 60°, and road adhesion coefficient of 0.8 or 0.6 is shown in Figures 7(a)–7(d).

The lateral displacement of the truck appears to increase as crosswind speed, truck speed, and wind angle increase. Truck speed has the greatest impact on lateral displacement among these factors, which may be due to the effects of the road power spectrum on the vehicle's stability. Figures 7(a)–7(d) also show that the road adhesion coefficient has the smallest effect on the lateral displacement of the truck among the factors simulated here, possibly because the truck is dry ($\varphi = 0.8$) or slippery ($\varphi = 0.6$) under the simulation conditions. The lateral force of the truck subjected to crosswinds did not reach the limit of the cornering force that the tires can provide, so lateral instability did not occur.

Table 1: Truck parameters.

Variable	Parameter	Unit
l_a	1110	mm
l_b	4775	mm
h_{cg}	1175	mm
W	2438	mm
A_v	10	m^2
m_c	6545	kg
k_s	250	N/mm
C	15	$KN{\cdot}s{\cdot}m^{-1}$
k_1	5228.8	N/deg
k_2	5228.8	N/deg
I_{xx}	2286.8	$kg{\cdot}m^2$
I_{yy}	35408.7	$kg{\cdot}m^2$
I_{zz}	34823.2	$kg{\cdot}m^2$
I_{xz}	1626	$kg{\cdot}m^2$
ρ_{air}	1.206	$kg{\cdot}m^{-3}$
Φ	0.2, 0.4, 0.6, 0.8	—

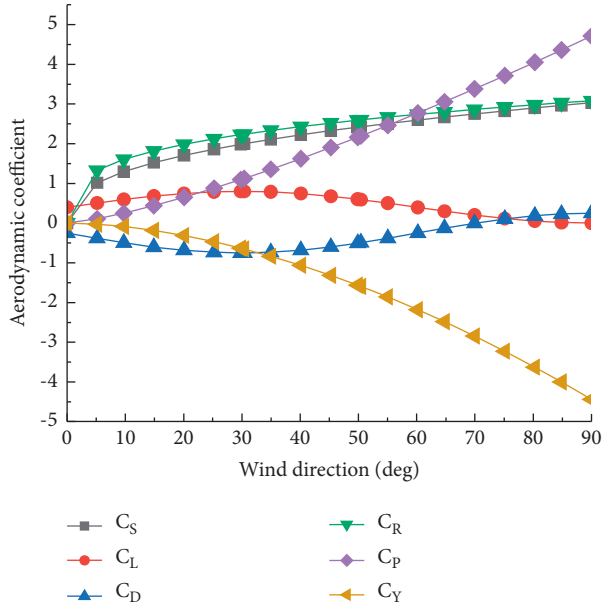

Figure 4: Aerodynamic parameters of truck varying with the wind direction.

4.4. Truck Heading Angle under Crosswind Conditions. According to the vehicle rotation accident standard [7], when the yaw angle of the vehicle exceeds 0.2 rad, a rotation accident can be considered to have occurred. As shown in Figure 8, when the truck moves down a dry road ($\varphi = 0.8$) at a constant speed of 108 kph, the pulsating average wind speed is $10\,m{\cdot}s^{-1}$, $20\,m{\cdot}s^{-1}$, $30\,m{\cdot}s^{-1}$, or $40\,m{\cdot}s^{-1}$, while pulsating crosswinds have an angle of 60°.

Fluctuations in heading angle appear to increase as the average pulsating wind speed increases. These fluctuations are maximal, when the average crosswind speed is 40 m·s-1, and fall into order from most intense to least intense at $40\,m{\cdot}s^{-1}$, $30\,m{\cdot}s^{-1}$, $20\,m{\cdot}s^{-1}$, and $10\,m{\cdot}s^{-1}$, respectively. When only the crosswind speed is changed, the heading angle changes are synchronized with the crosswind speed change trend. The crosswinds applied in the simulation are pulsating and thus have strong volatility, which caused the truck heading angle to change as the pulsating wind direction changed.

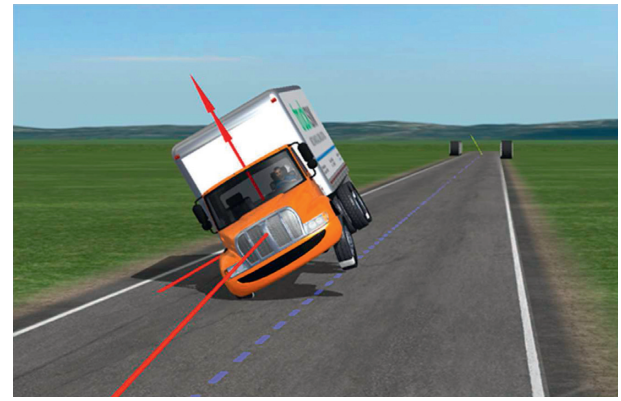

Figure 5: The road vehicle rolls over.

5. Importance Sampling Fuzzy Random Method

Monte Carlo simulation is a commonly used method for processing system reliability problems. Its premise is to simulate the failure probability of a small probability event over a large amount of available data, which can make it costly to operate and relatively inaccurate. Technical means of improving the Monte Carlo method's efficacy include importance sampling and reduced variance. Importance sampling technology is often used as it has relatively low computational cost and high accuracy [44].

Therefore, this paper also uses importance sampling technology to improve the performance of Monte Carlo simulation. The importance density function $h_x(X)$ must be introduced to operate the importance sampling method, where formula (10) changes to

$$P_f = \int_{R^n} \mu_E[g_x(X)] \frac{f_x(X)}{h_x(X)} h_x(X) \mathrm{d}x = E_s\left([g_x(X)] \frac{f_x(X)}{h_x(X)} \right). \tag{41}$$

The importance distribution function should be treated as having the most probable point (MPP). Carrarini [29] described the use of the first-order reliability method (FORM) to calculate MPP. The estimated value of the failure probability function is calculated as follows:

$$\widehat{P}_f = \frac{1}{M} \sum_{i=1}^{M} \mu_E[g_x(x_i)] \frac{f_x(x_i)}{h_x(x_i)}, \tag{42}$$

where $x_i (i = 1, 2, \ldots, M)$ represents the M sampling points obtained according to the distribution function $h_x(X)$.

Reliability sensitivity is defined by the partial derivative of the failure probability with respect to the distribution parameters of basic variables (e.g., mean and standard deviation), which can be determined according to formula (44).

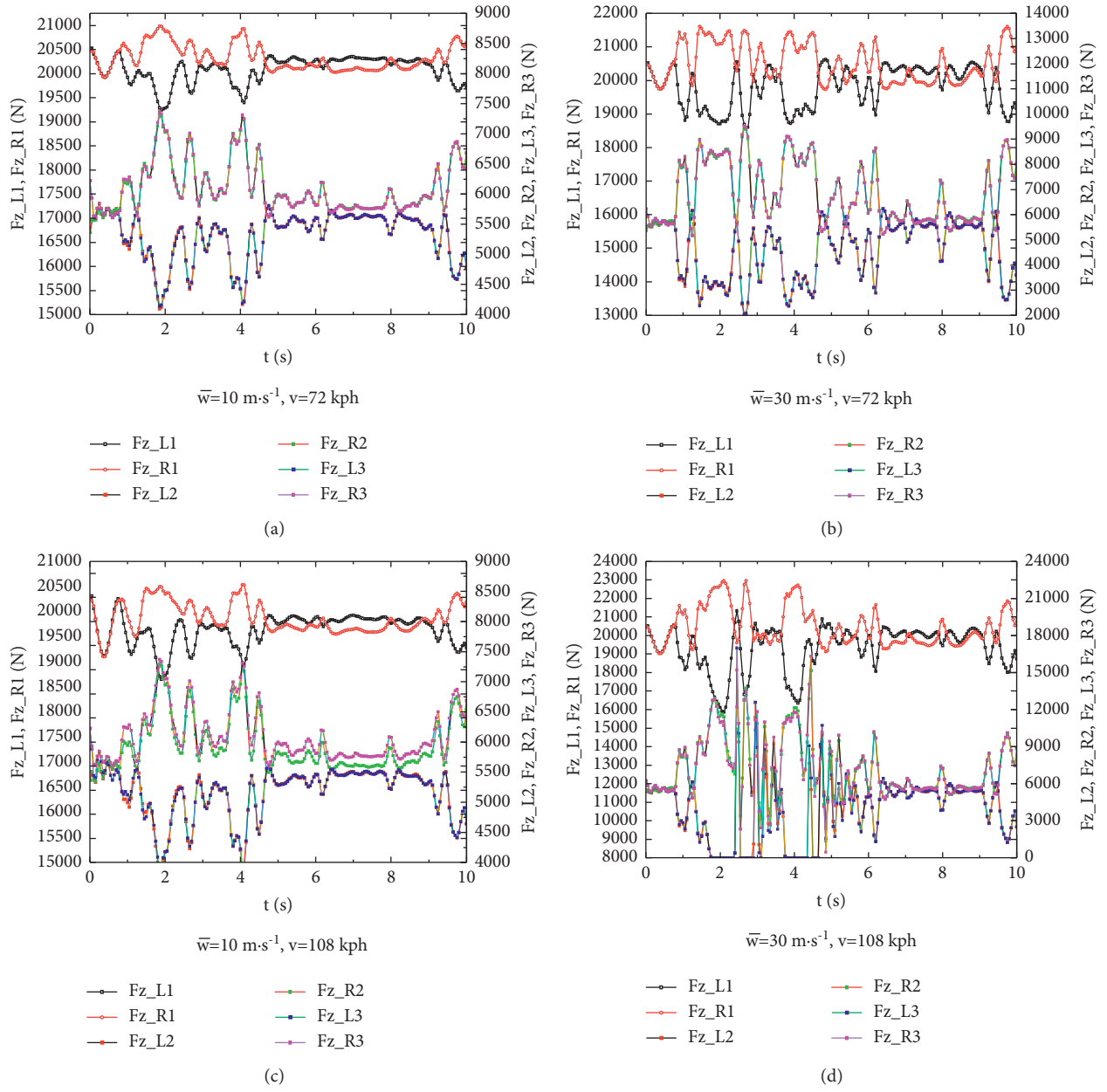

Figure 6: Time history curve of truck tire vertical load. (a) $\overline{w} = 10\,\mathrm{m} \times \mathrm{S}^{-1}, V = 72\,\mathrm{kph}$. (b) $\overline{w} = 30\,\mathrm{m} \times \mathrm{S}^{-1}, V = 72\,\mathrm{kph}$. (c) $\overline{w} = 10\,\mathrm{m} \times \mathrm{S}^{-1}, V = 108\,\mathrm{kph}$. (d) $\overline{w} = 30\,\mathrm{m} \times \mathrm{S}^{-1}, V = 108\,\mathrm{kph}$.

$$\frac{\partial P_f}{\partial \mu_{x_i}} = \int_{R^n} \mu_E \frac{[g_x(X)]}{h_x(X)} \frac{\partial f_x(X)}{\partial \mu_{x_i}} h_x(X)\mathrm{d}x = E_s\left(\frac{\mu_E[g_x(X)]}{h_x(X)} \frac{\partial f_x(X)}{\partial \mu_{x_i}}\right). \tag{43}$$

The importance sampling technique can be used to estimate the distribution parameter of the basic variable according to formula (43).

$$\frac{\partial \widehat{P}_f}{\partial \mu_{x_i}} = \frac{1}{M} \sum_{i=1}^{M} \mu_E \frac{[g_x(X)]}{h_x(X)} \frac{\partial f_x(X)}{\partial \mu_{x_i}} h. \tag{44}$$

6. Simulation Calculation and Analysis

The fuzzy stochastic method was used as described above to analyze truck stability under crosswind conditions at truck speeds of 72 kph, 90 kph, 108 kph, 126 kph, and 144 kph with average crosswind speeds of 10 $\mathrm{m{\cdot}s^{-1}}$, 20 $\mathrm{m{\cdot}s^{-1}}$, 30 $\mathrm{m{\cdot}s^{-1}}$, and 40 $\mathrm{m{\cdot}s^{-1}}$. The road adhesion coefficient as set to $\varphi = 0.6$ and the wind angle to 90°. The importance sampling method and fuzzy random method were used to analyze the stability of three-axle trucks and FPSS (including side-slip accidents, rotating accidents, and rollover accidents), as shown in Figure 9.

As shown in Figure 9, when the truck is traveling at a constant speed, FPSS increases as the average pulsating wind

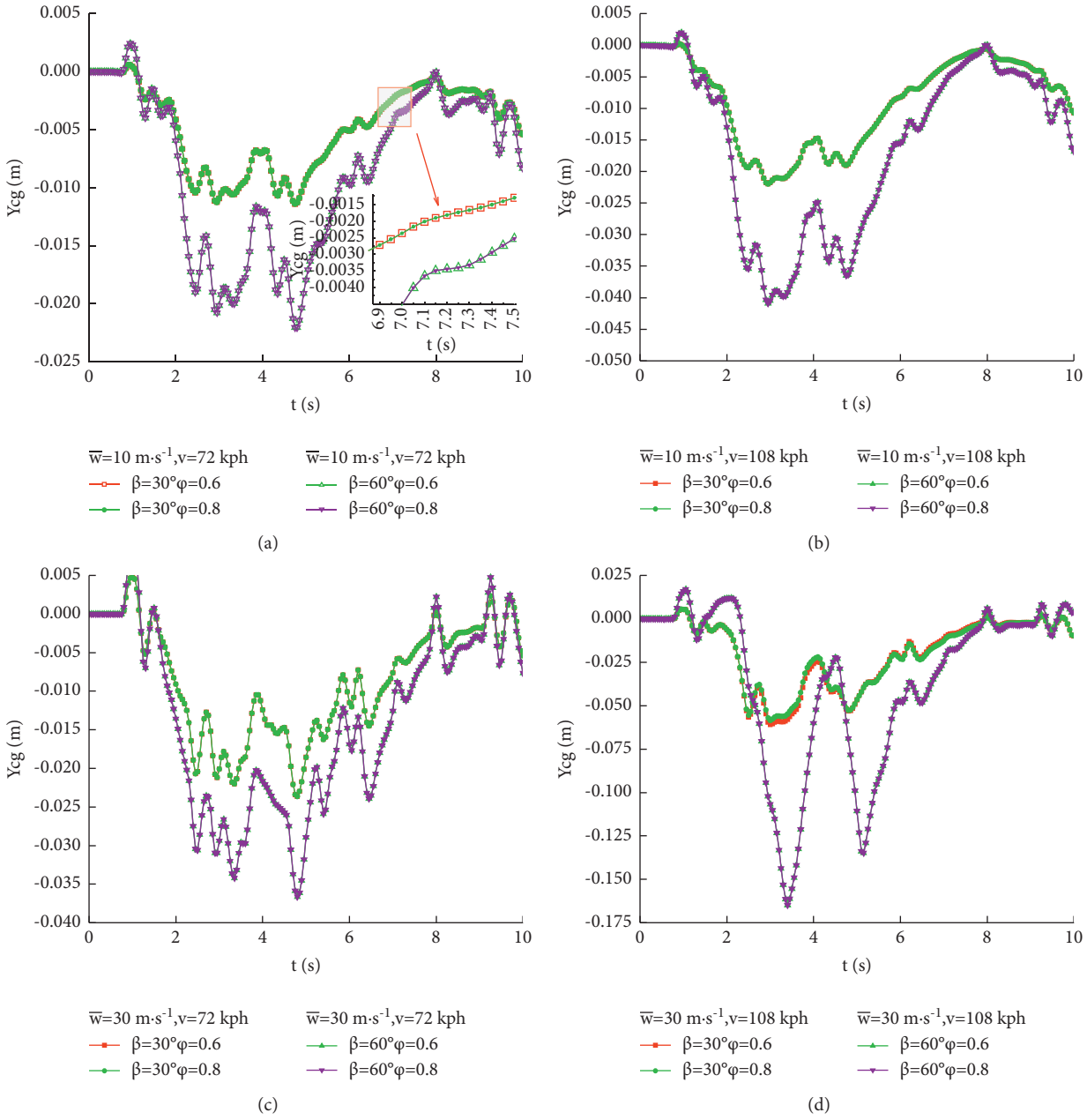

Figure 7: Time history curve of truck lateral displacement.

speed increases. The failure (accident) mode of the truck is affected by its speed. Under the combined action of fluctuating wind and truck speed, FPSS increases significantly. For example, when the fluctuating wind is 20 m·s^{-1} and the truck travels at 90 kph, FPSS is Pf1 = 0.003016718. When fluctuating wind is 30 m·s^{-1} and the truck travels at 90 kph, the FPSS is Pf2 = 0.004701093. When pulsating wind is 20 m·s^{-1} and truck speed is 108 kph, FPSS is Pf3 = 0.009815781; when pulsating wind is 30 m·s^{-1} and truck speed is 108 kph, FPSS is Pf4 = 0.021305156. The superposition of truck travel speed and the average pulsating wind speed significantly affects accident probability. Trucks should travel as slowly as possible under elevated pulsating wind speeds to minimize the probability of failure.

Trucks may experience side-slip, rotation, and (or) rollover accidents. Any one of these can constitute a series structure system. The sensitivity of the basic variables when the truck travels at 108 kph in pulsating crosswinds is shown in Figure 10. LTR has the greatest impact on accident probability among the variables observed here, followed by the truck yaw rate (RR) and finally the side-slip rate (RS). When the average pulsating crosswind speed is less than 20 m·s^{-1}, the sensitivity of the three random variables increases rapidly as the average pulsating crosswind speed increases. RR and RS reach their maximum values at 20 m·s^{-1}, indicating that the truck is most likely to rotate and/or experience side-slip accident under this pulsating average wind speed. When the average pulsating wind speed

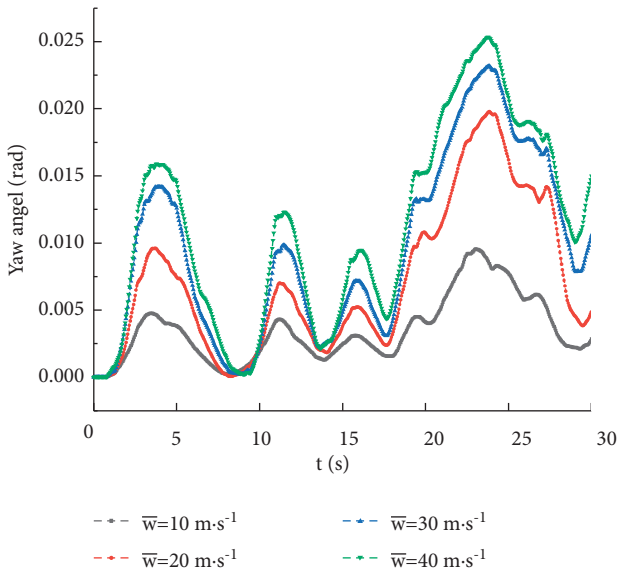

Figure 8: Time history curve of truck heading angle.

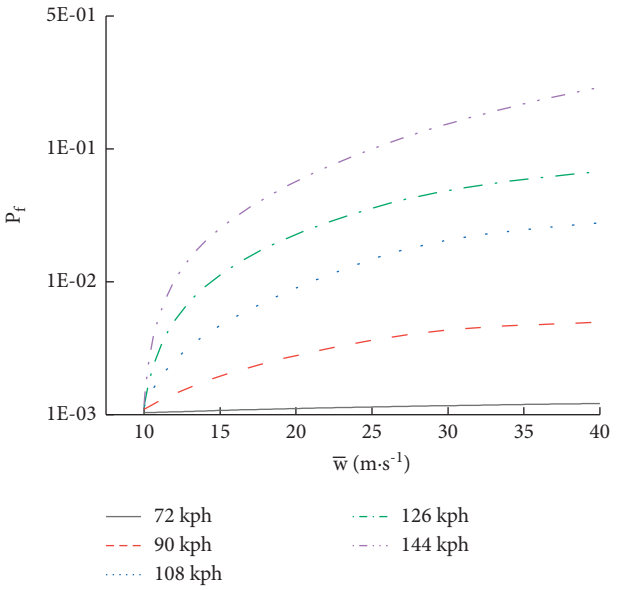

Figure 9: FPSS under different driving conditions.

exceeds 20 m·s^{-1}, the sensitivity of RR and RS to the probability of truck accidents is greatly reduced, while that of LTR continues to increase slowly, indicating that the primary mode of truck accidents after this point was rollover.

Yu et al. [31] proved that characteristic wind curves (CWCs) are more conservative than probabilistic characteristic wind curves (PCWCs). PCWCs were used in this study to operate the fuzzy random reliability method to evaluate the serial system of trucks with the potential for side-slip, rotation, or rollover accidents [7]. A 20% safety margin was reserved for the three accident indicators; that is, when the lateral displacement of the truck reached 0.4 m, the heading angle of the truck reached 0.16 rad, or LTR reached 0.8, the truck was considered to be at the boundary of the accident.

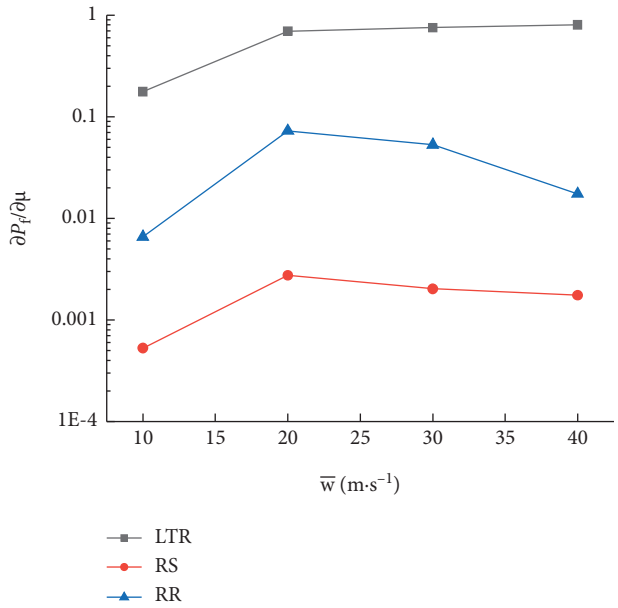

Figure 10: Variable sensitivity analysis.

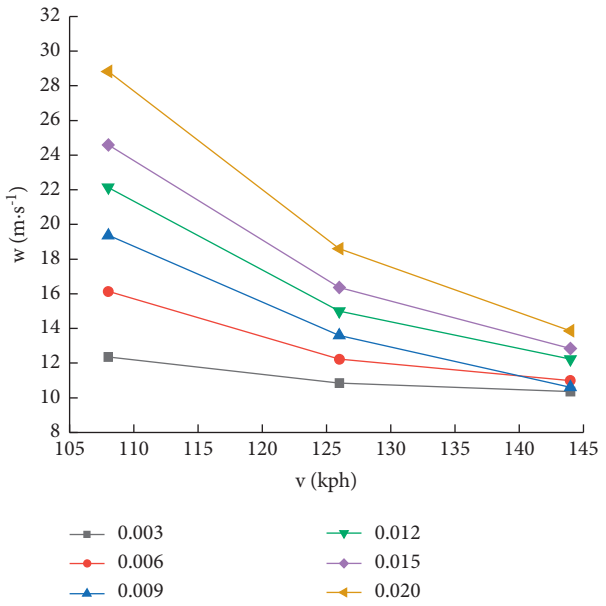

Figure 11: Safety critical speed.

The critical safe speed of the truck under a certain accident probability and pulsating average crosswind speed was determined as shown in Figure 11. The critical safety speed appears to decrease as pulsating crosswind speed increases under certain accident probabilities. Accident probability increases when the truck is running at a certain speed. When the truck travels at 108 kph and the pulsating wind speed changes from 22 m·s^{-1} to 29 m·s^{-1}, the accident probability of the truck rises rapidly from 0.012 to 0.020. The truck driver must slow his or her speed as quickly as possible upon encountering pulsating crosswinds in order to prevent an accident.

7. Conclusion

Previous studies have shown that deterministic CWC calculation results are extremely conservative. Crosswinds have strong uncertainty; previous scholars, however, have generally considered crosswind models to have steady states. Harmonic superposition was utilized in the present study to obtain a pulsating crosswind model. The random fuzzy method was used based on the reliability theory to analyze side-slip, rotation, and rollover accident probabilities under crosswind conditions. An FPSS calculation was conducted to expand on the previously reported failure probabilities of single accident types.

Wind angles, crosswind speed, truck speed, and road adhesion coefficients were used as random variables to explore truck accident probabilities. The load change of the front axle of the truck is not significantly affected by the side winds relative to the rear axle. Further, the influence of vehicle speed on axle load is relatively small compared to the influence of crosswinds. The lateral displacement of the truck is also affected by many factors. Among the four influencing factors considered here, truck speed has the greatest impact on lateral displacement. When truck drivers encounter crosswinds, they should reduce their speed as much as possible to ensure their safety.

The sensitivity of three indicators to truck accidents was analyzed to find that they fall into descending order as LTR, RR, and RS. Rollover accidents accounted for the largest proportion of truck failures in the simulation followed by rotation accidents and finally side-slip accidents. Indicator sensitivity was highest when the average pulsating crosswind speed was $20\,\mathrm{m{\cdot}s^{-1}}$, where parameter changes near the extreme point merit the most attention. The critical safety speed of trucks under different average wind speeds of pulsating crosswind was determined as a workable reference for road transportation safety management departments.

A framework was established in this study for calculating truck rollover, rotation, and/or slide-slip accident FPSS. The random fuzzy method was used to conduct a systematic evaluation of truck failures. The results of this work may provide a useful reference in addition to mitigating shortcomings of the WCW methods used in previous studies for the benefit of future researchers.

There are still many factors that affect the safe driving of a truck under crosswind conditions that were not taken into consideration here (e.g., road surface unevenness and driver's skills/experience). These factors may be considered in the future. Truck aerodynamics are also not fully understood and yet merit further research. Future scholars may provide verifications of the proposed calculation framework to strengthen its efficacy.

Data Availability

The data used to support the findings of the study are available from the corresponding author upon request.

Conflicts of Interest

The authors declare that they have no conflicts of interest.

Acknowledgments

This work was financially supported by the National Key Research and Development Program "integrated transportation and intelligent transportation" key special project "road transport network operation risk proactive prevention and control key technologies and applications" (2019YFB1600500).

References

[1] S. R. Chen and F. Chen, "Simulation-based assessment of vehicle safety behavior under hazardous driving conditions," *Journal of Transportation Engineering-asce*, vol. 136, 2010.

[2] X. Zhang and C. Proppe, "Risk assessment of road vehicles under wind gust excitation," *ASME Journal Computer Nonlinear Dynamics*, vol. 15, no. 10, Article ID 101004, 2020.

[3] R. Young, E. Offei, and Q. Dai, "High wind warning system for bordeaux," Report No. FHWA-WY-10 F 5, Department of Civil and Architectural Engineering, University of Wyoming, Laramie, Wyoming, 2010.

[4] J. McCarthy, "Evaluation of Intelligent Transportation System Alternatives for Reducing the Risks of Truck Rollover Crashes Due to High Winds," *U.S. Department of Transportation*, Federal Highway Administration, Cheyenne, WY, USA, Report No. FHWA-WY-07/01F, 2006.

[5] Y. Yang, L. Yang, B. Wu, G. Yao, H. Li, and S. Robert, "Safety prediction using vehicle safety evaluation model passing on long-span bridge with fully connected neural network," *Advances in Civil Engineering*, vol. 2019, Article ID 8130240, p. 12, 2019.

[6] S.-J. Kim, C.-H. Yoo, and H.-K. Kim, "Vulnerability assessment for the hazards of crosswinds when vehicles cross a bridge deck," *Journal of Wind Engineering and Industrial Aerodynamics*, vol. 156, pp. 62–71, 2016.

[7] C. J. Baker, "Measures to control vehicle movement at exposed sites during windy periods," *Journal of Wind Engineering and Industrial Aerodynamics*, vol. 25, no. 2, pp. 151–161, 1987.

[8] Z. Chen, K. T. Tse, K. C. S. Kwok, A. Kareem, and B. Kim, "Measurement of unsteady aerodynamic force on a galloping prism in a turbulent flow: a hybrid aeroelastic-pressure balance," *Journal of Fluids and Structures*, vol. 102, Article ID 103232, 2021.

[9] Z. Chen, H. Huang, Y. Xu, K. T. Tse, B. Kim, and Y. Wang, "Unsteady aerodynamics on a tapered prism under forced excitation," *Engineering Structures*, vol. 240, Article ID 112387, 2021.

[10] Z. Chen, X. Fu, Y. Xu, C. Y. Li, B. Kim, and K. T. Tse, "A perspective on the aerodynamics and aeroelasticity of tapering: partial reattachment," *Journal of Wind Engineering and Industrial Aerodynamics*, vol. 212, Article ID 104590, 2021.

[11] P. Hu, Y. Han, C. S. Cai, W. Cheng, and W. Lin, "New analytical models for power spectral density and coherence function of wind turbulence relative to a moving vehicle under crosswinds," *Journal of Wind Engineering and Industrial Aerodynamics*, vol. 188, pp. 384–396, 2019.

[12] C. J. Baker, "A simplified analysis of various types of wind-induced road vehicle accidents," *Journal of Wind Engineering and Industrial Aerodynamics*, vol. 22, no. 1, pp. 69–85, 1986.

[13] C. J. Baker, "High sided articulated road vehicles in strong cross winds," *Journal of Wind Engineering and Industrial Aerodynamics*, vol. 31, no. 1, pp. 67–85, 1988.

[14] S. R. Chen and C. S. Cai, "Accident assessment of vehicles on long-span bridges in windy environments," *Journal of Wind Engineering and Industrial Aerodynamics*, vol. 92, no. 12, pp. 991–1024, 2004.

[15] C. S. Cai and S. R. Chen, ""Framework of vehicle–bridge–wind dynamic analysis," *Journal of Wind Engineering and Industrial Aerodynamics*, vol. 92, no. 7-8, pp. 579–607, 2004.

[16] H. Yu, B. Wang, Y. Li, and M. Zhang, "Driving risk of road vehicle shielded by bridge tower under strong crosswind," *Natural Hazards*, vol. 96, no. 1, pp. 497–519, 2019.

[17] X. Zhang and C. Proppe, "The influence of strong crosswinds on safety of different types of road vehicles," *Meccanica*, vol. 54, no. 9, pp. 1489–1497, 2019.

[18] Z. Xiong, J. Zhu, K. Zheng, W. Zhang, Y. Li, and M. Wu, "Framework of wind-traffic-bridge coupled analysis considering realistic traffic behavior and vehicle inertia force," *Journal of Wind Engineering and Industrial Aerodynamics*, vol. 205, Article ID 104322, 2020.

[19] C. Feng and S. Chen, "Reliability-based assessment of vehicle safety in adverse driving conditions," *Transportation Research Part C: Emerging Technologies*, vol. 19, no. 1, pp. 156–168, 2011.

[20] P. Teufel, *Böenmodellierung und lastabminderung für ein flexibles flugzeug*, Ph.D. thesis, University of Stuttgart, Stuttgart, Germany, 2003.

[21] G. C. Larsen, W. Bierbooms, and K. S. Hansen, "Mean gust shapes," Report No. RISO-R1133, Risoe National Lab., Roskilde, Denmark, 2003.

[22] P. Gautier, T. Tielkes, F. Sourget et al., "Strong wind risks in railways: the DEUFRAKO crosswind program," in *Proceedings of the World Congress of Railway Research (WCRR)*, pp. 463–475, Edinburgh, Scotland, August 2003.

[23] L. M. Cleon and A. Jourdain, "Protection of line LN5 against cross winds," in *Proceedings of the Fifth World Congress on Railway Research*, koeln, Germany, November 2001.

[24] M. Yu, J. Zhang, K. Zhang, and W. Zhang, "Crosswind stability analysis of a high-speed train based on fuzzy random reliability," *Proceedings of the Institution of Mechanical Engineers - Part F: Journal of Rail and Rapid Transit*, vol. 229, no. 8, pp. 875–887, 2015.

[25] J. Snæbjornsson, C. Baker, and R. Sigbjornsson, "Probabilistic assessment of road vehicle safety in windy environments," *Journal of Wind Engineering and Industrial Aerodynamics*, vol. 95, no. 9–11, pp. 1445–1462, 2007.

[26] C. Wetzel and C. Proppe, "On reliability and sensitivity methods for vehicle systems under stochastic crosswind loads," *Vehicle System Dynamics*, vol. 48, no. 1, pp. 79–95, 2010.

[27] X.-m. Shao, J. Wan, D.-w. Chen, and H.-b. Xiong, "Aerodynamic modeling and stability analysis of a high-speed train under strong rain and crosswind conditions," *Journal of Zhejiang University - Science*, vol. 12, no. 12, pp. 964–970, 2011.

[28] W. Bierbooms and P.-W. Cheng, "Stochastic gust model for design calculations of wind turbines," *Journal of Wind Engineering and Industrial Aerodynamics*, vol. 90, no. 11, pp. 1237–1251, 2002.

[29] A. Carrarini, "Reliability based analysis of the crosswind stability of railway vehicles," *Journal of Wind Engineering and Industrial Aerodynamics*, vol. 95, no. 7, pp. 493–509, 2007.

[30] M. Yu, J. Zhang, and W. Zhang, "Simulation of unsteady aerodynamic loads on high-speed trains in fluctuating crosswinds," *Journal of Modern Transportation*, vol. 21, no. 2, pp. 73–78, 2013.

[31] M. Yu, J. Zhang, and W. Zhang, "Operational safety reliability of high-speed trains under stochastic winds," *Chinese Journal of Theoretical and Applied Mechanics*, vol. 45, no. 4, pp. 483–492, 2013.

[32] C. J. Baker, "Unsteady wind loading on a wall," *Wind and Structures*, vol. 4, no. 5, pp. 413–440, 2001.

[33] M. Sterling, C. J. Baker, P. J. Richards, R. P. Hoxey, and A. D. Quinn, "An investigation of the wind statistics and extreme gust events at a rural site," *Wind and Structures*, vol. 9, no. 3, pp. 193–215, 2006.

[34] C. Baker, "A framework for the consideration of the effects of crosswinds on trains," *Journal of Wind Engineering and Industrial Aerodynamics*, vol. 123, pp. 130–142, 2013.

[35] R. K. Cooper, "Atmospheric turbulence with respect to moving ground vehicles," *Journal of Wind Engineering and Industrial Aerodynamics*, vol. 17, no. 2, pp. 215–238, 1984.

[36] B. S. En, *Railway applications Aerodynamics-Part 6: Requirements and test procedures for cross wind assessment*, European Standard, Brussels, Belgium, 2010.

[37] C. Wetzel and C. Proppe, "Crosswind stability of high-speed trains: a stochastic approach," in *Proceedings of the The BBAA VIth International Colloquium on bluff Bodies Aerodynamics & Applications*, Milano, Italy, July 2008.

[38] C. J. Baker, "The simulation of unsteady aerodynamic cross wind forces on trains," *Journal of Wind Engineering and Industrial Aerodynamics*, vol. 98, no. 2, pp. 88–99, 2010.

[39] B. Wang and Y.-L. Xu, "Safety analysis of a road vehicle passing by a bridge tower under crosswinds," *Journal of Wind Engineering and Industrial Aerodynamics*, vol. 137, pp. 25–36, 2015.

[40] Y. Zhou and S. Chen, "Fully coupled driving safety analysis of moving traffic on long-span bridges subjected to crosswind," *Journal of Wind Engineering and Industrial Aerodynamics*, vol. 143, pp. 1–18, 2015.

[41] J. Bendat and A. Piersol, *Random Data—Analysis and Measurement Procedures*, Wiley-Interscience, Hoboken, NJ, USA, 1977.

[42] S. A. Coleman and C. J. Baker, "High sided road vehicles in crosswind," *Journal of Wind Engineering and Industrial Aerodynamics*, vol. 36, pp. 1383–1392, 1990.

[43] Mechanical Simulation Corporation, *TruckSim User Manual*, Mechanical Simulation Corpo-ration, Ann Arbor, MI, USA, 2016.

[44] S. K. Au and J. L. Beck, "Important sampling in high dimensions," *Structural Safety*, vol. 25, no. 2, pp. 139–163, 2003.